
Geological Survey of Canada

CURRENT RESEARCH 2001-A8

# *New insights into metavolcanic successions and geochemistry of the Eagle Bay Assemblage, south-central British Columbia*

*S.L. Bailey, S. Paradis, and S.T. Johnston*

Natural Resources Canada | Ressources naturelles Canada

Canada

Catalogue No. M44-2001/A8E-IN
ISBN 0-662-29788-1

Available in Canada from the
Geological Survey of Canada Bookstore website at:
http://www.nrcan.gc.ca/gsc/bookstore (Toll-free: 1-888-252-4301)

A copy of this publication is also available for reference by depository libraries across Canada through access to the Depository Services Program's website at http://dsp-psd.pwgsc.gc.ca

Price subject to change without notice

# New insights into metavolcanic successions and geochemistry of the Eagle Bay Assemblage, south-central British Columbia[1]

**S.L. Bailey[2], S. Paradis, and S.T. Johnston[2]**
*Mineral Resources Division, Sidney*

*Bailey, S.L., Paradis, S., and Johnston, S.T., 2001: New insights into metavolcanic successions and geochemistry of the Eagle Bay Assemblage, south-central British Columbia; Geological Survey of Canada, Current Research 2001-A8, 16 p.*

[1] Contribution to the Ancient Pacific Margin NATMAP Project

[2] School of Earth and Ocean Sciences, University of Victoria, P.O. Box 3055, Station CSC, Victoria, British Columbia V8W 3P6

***Abstract:***

*The Eagle Bay Assemblage of the Kootenay Terrane in the Johnson and Adams lakes area comprises deformed, greenschist-facies sedimentary rocks and bimodal volcanic rocks. Two volcanic successions are present, an Upper Devonian mafic and felsic metavolcanic succession and a Lower Cambrian mafic metavolcanic succession. The latter is interbedded with archaeocyathid-bearing carbonate rocks. Upper Devonian U-Pb zircon ages of 360 ± 6 Ma have been obtained for felsic metavolcanic rocks of the bimodal succession.*

*Lithogeochemical analyses of the metavolcanic rocks have identified two distinct metabasic successions. Mafic metavolcanic rocks of the Upper Devonian bimodal succession are alkalic, whereas Cambrian mafic metavolcanic rocks are subalkaline. The mafic metavolcanic rocks of the bimodal alkalic succession are associated with base- and precious-metal occurrences, such as the Rea, Samatosum, and Homestake deposits.*

***Résumé :***

*L'Assemblage d'Eagle Bay du terrane de Kootenay dans la région des lacs Johnson et Adams se compose de roches sédimentaires déformées et métamorphisées au faciès des schistes verts et de roches volcaniques bimodales. Deux successions volcaniques sont présentes, une de roches métavolcaniques mafiques et felsiques du Dévonien supérieur et une autre de roches métavolcaniques mafiques du Cambrien inférieur. Cette dernière est interstratifiée avec des roches carbonatées à archéocyathidés. La datation U-Pb de zircons provenant des roches métavolcaniques felsiques de la succession bimodale a donné des âges de 360 ± 6 Ma (Dévonien supérieur).*

*Les analyses lithogéochimiques des roches métavolcaniques permettent de reconnaître deux successions distinctes de roches metabasiques. Les roches métavolcaniques mafiques de la succession bimodale du Dévonien supérieur ont une composition alcaline, alors que les roches métavolcaniques mafiques du Cambrien ont une composition subalcaline. Les roches métavolcaniques mafiques de la succession alcaline bimodale sont associées à des indices de métaux communs et de métaux précieux, tels les gisements Rea, Samatosum et Homestake.*

## INTRODUCTION

In 1999, 1:20 000 scale geological mapping was initiated as part of the Ancient Pacific Margin NATMAP Project in the Johnson and Adams lakes area, 80 km north of Kamloops (**Fig. 1**). Lower-middle greenschist facies bimodal volcanic and sedimentary rocks of the Eagle Bay Assemblage underlie the study area, which is part of the pericratonic Kootenay Terrane (Schiarizza and Preto, 1987). The area has significant potential for mineral exploration including massive sulphide-barite deposits (Rea, Homestake, K7) and high-grade quartz-carbonate-vein-hosted silver deposits (Samatosum).

The project has the following goals: 1) to produce a 1:20 000 scale geological map summarizing the stratigraphy and structure of the Johnson and Adams lakes area; 2) to examine the geochemistry of metavolcanic rocks; and 3) to examine the origin and metallogenesis of this pericratonic package of rocks. Bailey et al. (2000) summarized preliminary geological mapping and unit descriptions and reviewed several of the known mineral occurrences (Rea, Samatosum, Twin Mountain).

Here we present lithogeochemical data and interpretations of metavolcanic sequences that are associated with massive sulphide deposits in the Johnson and Adams lakes area. Petrochemical studies in volcanic-hosted massive-sulphide districts (e.g. Swinden, 1996; Lentz, 1996) have shown that metavolcanic rock geochemical signatures can provide insight into their paleotectonic setting and metallogenic evolution. Furthermore, these studies have shown that volcanic lithogeochemical signatures provide a guide to the exploration and discovery of new volcanic-hosted massive-sulphide mineralization.

## GEOLOGY

The Eagle Bay Assemblage in the Johnson and Adams lakes area is dominated by deformed, greenschist facies, metasedimentary and metavolcanic rocks that range from Lower Cambrian to Mississippian in age (Schiarizza and Preto, 1987). Previous geological mapping of the Eagle Bay Assemblage has been published at 1:250 000 scale by Okulitch (1979), and at 1:100 000 scale by Schiarizza and Preto (1987).

Units have been subdivided using the nomenclature of Schiarizza and Preto (1987), with the exception of the volcanic unit hosting the Homestake deposit, which has been grouped with unit EBFin. This is thought to be a variably hydrothermally altered package of dominantly mafic to intermediate composition

and may be a structural repetition of Devonian metabasite to the east (**Fig. 2**). This hypothesis will be tested with future lithogeochemical data. Lithogeochemical data have been obtained for units EBG, EBFmv, EBFin, and EBFfv, and this report focuses on preliminary results for each of these units east of the Homestake deposit.

Unit EBG is a greenschist and greenstone package intercalated with marble (EBGt) and metasedimentary rocks (EBGs). It is generally melanocratic, massive with tuffaceous interbeds, has abundant epidote and quartz veins containing a fibrous mineral ((?)amphibole). The marble has been correlated to the archaeocyathid-bearing Tshinakin Limestone, which outcrops near Vavenby, and constrains this package to a Lower Cambrian age.

A mafic metavolcanic package (EBFmv) forms the structural hanging wall of the Samatosum quartz-vein-hosted silver deposit, and the Rea and K7 massive sulphide-barite deposits (Bailey et al., 2000). This package of rocks consists of greenschist and greenstone derived from mafic fragmental volcanic rocks, flows, and tuff. The dominant mineral assemblage consists of chlorite, actinolite, plagioclase, ankerite, siderite, quartz, pyrite, and magnetite.

Unit EBFin consists of greenschist- and greenstone-derived metavolcanic and metavolcaniclastic rocks of intermediate composition, with minor felsic and mafic components that outcrop in the central part of the map area (Fig. 2). The mineral assemblages consist of chlorite, plagioclase, ankerite, siderite, sericite, quartz, and pyrite.

Quartz-sericite-ankerite schist interpreted as felsic metavolcanic rocks (EBFfv) outcrop in the hinge zone of an overturned syncline, making it the youngest of the volcanic units described herein. Preserved igneous textures include phenocrysts of quartz and feldspar as well as monolithic felsic fragments. The matrix has been altered to sericite, quartz, and ankerite with minor pyrite. Recent U-Pb zircon dating

suggests an Upper Devonian crystallization age (360 ± 6 Ma) for unit EBFfv and identified the presence of an Upper Proterozoic (750.4 ± 158.4 Ma) xenocryst (L. Heaman, pers. comm, 2000). Previous U-Pb zircon dating yielded ages of 387 Ma for felsic metavolcanic rocks from the east side of Adams Lake (Schiarizza and Preto, 1987).

Unit distribution is controlled by two major structures, the Haggard Creek Thrust Fault, which places Lower Cambrian rocks over Devonian–Mississippian rocks, and an overturned syncline that occurs in the footwall of the fault. Both are northwest-trending, southwest-verging structures. An axial planar schistosity defined by metamorphic mineral grains indicates that metamorphism was synkinematic (Schiarizza and Preto, 1987).

## GEOCHEMICAL ANALYSIS

### *Methodology*

Sampling for whole-rock geochemical (major and trace elements) and petrographical analyses was conducted in 1999 (120 samples) and 2000 (55 samples). Samples submitted for geochemical analysis are representative of the units, homogeneous, and lack fragments, veins, and large individual crystals. The goal of the lithogeochemical analysis is to ascertain regional geochemical characteristics of the units, investigate alteration zones associated with massive-sulphide mineralization, and provide insights into the tectonic setting(s) of volcanism. Detailed petrographic studies of the volcanic rocks were carried out in conjunction with field mapping to identify mineral assemblages, textural variability among alteration types, and paragenetic relationships.

One hundred and twenty samples were submitted to the Geological Survey of Canada's Analytical Chemistry Laboratories for whole-rock geochemical analysis by fused disk wavelength, dispersive X-ray fluorescence, and acid dissolution ICP-MS, ICP-ES. Further information on sample preparation, X-ray fluorescence, ICP-MS, and ICP-ES analysis can be found in Jenner et al. (1990), Rollinson (1993), and Longerich (1995).

## *Alteration and metamorphism*

Field and petrographic examination of the samples from this study show that regional greenschist-facies metamorphism is indicated by the presence of a well developed schistosity defined by chlorite, muscovite, actinolite, and biotite. The presence of localized alteration zones related to volcanic-hosted massive-sulphide deposit formation suggest that seafloor hydrothermal metamorphism was penecontemporaneous with eruption. Metabasic rocks have assemblages of chlorite, epidote, actinolite, plagioclase, Fe-carbonate, sericite, ±pyrite, and magnetite. Felsic metavolcanic rocks have metamorphic assemblages of quartz, feldspar, sericite, Fe carbonates, and pyrite. Metasedimentary rocks have assemblages of sericite, chlorite, quartz, feldspar, Fe-carbonates, aluminosilicates, and pyrite.

Primary volcanic and sedimentary features are observed in the area. In the mafic to intermediate metavolcanic rocks, these include fragmental textures, chilled rims of pillows, and plagioclase phenocrysts. The metafelsic rocks retain primary quartz and plagioclase phenocrysts and fragmental textures. Graded bedding, scour-and-fill structures, and rip-up clasts are preserved in the metasedimentary units and are interpreted to represent turbidite sequences (Höy and Goutier, 1986).

## PRELIMINARY RESULTS

Because of metamorphism and alteration of the metavolcanic rocks, major-element classifications are suspect. Therefore, diagrams using high field-strength elements (HFSE; Zr, Nb, Y, Ti, Hf, Ta) were used to classify rocks.

Trace-element discrimination diagrams (**Fig. 3a**) indicate that unit EBFmv has an alkalic affinity (NB/Y<0.7), units EBFfv and EBF have a transitional alkalic-subalkalic character, and unit EBG has a subalkalic affinity (NB/Y<0.7). This distinction cannot be made using the $SiO_2/(Zr/TiO_2)$ discrimination diagram (**Fig. 3b**) of Winchester and Floyd (1977).

Discrimination diagrams based on alkali elements, magnesium, iron and silica, yield inconsistent results. For example mafic rocks of units EBG and EBFmv straddle the 'calkalkaline-tholeiite' field of Irvine and Baragar (1971) (**Fig. 3c**) and the subalkaline-alkaline field of Irvine and Baragar (1971) (**Fig. 3d**). Additions of K and Na due to the presence of sericite result in these samples crossing the discrimination-diagram boundaries.

Normalized multielement plots were designed using the normalization values of Sun and McDonough (1989) to examine incompatible-element patterns. Elements are organized from left to right in order of decreasing incompatibility in a mantle source region. Incompatible elements have a distribution coeffiecient (KD = concentration of element in mineral / concentration in melt) less than 1 (Rollinson, 1993). Incompatible elements prefer the melt phase and are increasingly concentrated in the melt as crystallization occurs. The behaviour of elements can change from incompatible to compatible if a phase crystallizes for which that element has high affinity. For example in a felsic system, zirconium (Zr)

becomes compatible as zircon crystallizes. Concentrations of elements reflect the composition of source regions, temperatures and pressures of melting, oxygen activity, crystal chemistry, and water content of the magma (Rollinson, 1993).

A chondrite-normalized rare-earth-element plot (**Fig. 3e**) shows that meta-igneous rocks of unit EBF are enriched in light rare earth elements (LREE) relative to heavy rare earth elements (HREE). Patterns for units EBFmv, EBFin, and EBFfv are similar. Units EBFin and EBFfv have higher absolute abundances of LREEs. Metabasite of unit EBG is characterized by depleted LREEs relative to the HREEs.

A primitive-mantle-normalized incompatible multielement plot (**Fig. 4a**) is used to demonstrate the geochemical variation between units EBFmv, EBFin, and EBFfv. These include negative Nb anomalies relative to Th and La, and negative Ti anomalies relative to Eu and Gd. The remainder of the incompatible elements display parallel trends with enrichments of highly incompatible elements relative to compatible elements. Unit EBG is depleted in highly incompatible elements relative to less incompatible elements.

Samples were normalized to an average N-MORB composition (**Fig. 4b**) to test the nature of the magma source region. Any magmatic product derived from a depleted-mantle source, with no crustal contamination or subducting slab influence, should display a flat incompatible-element pattern (Rollinson, 1993). Unit EBF metavolcanic rocks are enriched in highly incompatible elements. Unit EBG metabasite is characterized by flat patterns consistent with derivation from a depleted-mantle source.

Yttrium and zirconium behave in an incompatible fashion (Jenner, 1996) and volcanic rocks from the same magmatic event should have comparable Y/Zr ratios. These Y/Zr ratios differ for units EBFmv, EBFin, EBFfv, and EBG. Unit EBFmv has Y/Zr ratios of 0.25, and units EBFin and EBFfv have Y/Zr ratios of approximately 0.15. Unit EBG metabasite has higher Y/Zr ratios of approximately 0.9.

## TECTONIC DISCRIMINATION DIAGRAMS

The tectonic discrimination diagram (**Fig. 4d**) of Pearce and Cann (1973) uses the high field-strength elements (HFSE) Zr, Y, and Ti to classify basalts. Unit EBFmv samples plot in the 'within-plate' basalt field whereas unit EBG metabasite plots outside the 'tholeiite' field. Samples plotted on the tectonic discrimination diagrams of Wood (1980) (**Fig. 5a, b**) display two distinct trends. Unit EBFmv metabasite plots in the alkalic within-plate basalt field, whereas unit EBG metabasite plots in the normal mid-ocean-ridge basalt field.

The Nb/Y discrimination plot (**Fig. 5c**) of Pearce et al. (1984) uses this ratio to discriminate felsic rock types and is biased toward granitoid rocks. Felsic rocks of the Johnson and Adams lakes area straddle the boundary between within-plate and arc-related volcanism, with Nb values ranging from 10 to 25 ppm and Y values, from 15 to 39 ppm.

The discrimination diagram of Shervais (1982) (**Fig. 5d**) is based on differences in behaviour between transition elements Ti and V reflecting the oxidation state of the magma. Vanadium can exist in three oxidation states ($V^{3+}$, $V^{4+}$, and $V^{5+}$), which have varied partition coeffiecients for pyroxene and magnetite; titanium only exists as $Ti^{4+}$ (Rollinson, 1993). In oxidized systems (magmatic arcs), vanadium is less compatible in these minerals and fractionates into the melt, leading to enrichments in V relative to Ti. Unit EBFmv has V/(Ti/1000) ratios of approximately 50, whereas unit EBG has V/(Ti/1000) ratios of approximately 20 and straddles the arc–ocean floor basalt boundary.

Meschede (1986) used the immobile incompatible elements Nb, Y, and Zr to distinguish basalt types. Samples of unit EBFmv plot in the within-plate basalt field (**Fig. 5e**) and samples of unit EBG plot outside the volcanic arc basalt–mid-ocean-ridge basalt field.

## DISCUSSION

The primitive-mantle-normalized spider diagram (**Fig. 4a**) illustrates that an apparent negative Nb and Ti anomaly in the intermediate (EBFin) and felsic (EBFfv) packages appears to be balanced by a slight positive anomaly in genetically related mafic volcanic rocks (EBFmv). Negative Nb and Ti anomalies in mafic rocks are characteristic of volcanic arcs (Rollinson, 1993). However, in intermediate to felsic systems, this anomaly may be controlled by crystallization of a titanomagnetite phase in the restite, and is independent of tectonic setting (Christiansen and Keith, 1996).

The Y/Zr ratios (**Fig. 4c**) show a possible differentiation trend for unit EBF, suggesting bimodal volcanism, in addition to defining two different magmatic events within the region. The Y/Zr ratio difference in units EBFmv, EBFin, and EBFfv can be explained by the behaviour of zirconium. In a felsic melt the ratio changes as Zr becomes compatible and zircon crystallizes.

Unit EBG has characteristics of mid-ocean-ridge basalt (MORB). In particular the flat patterns displayed by the incompatible elements when normalized to average MORB composition (**Fig. 4b**) indicate that it is derived from a depleted-mantle source. We interpret this to represent volcanism in an evolved marginal basin setting. These rocks show no evidence of contamination by continental crustal material. If this represents Lower Cambrian rifting of the Western North American margin, it is possible that extension had thinned the crust sufficiently to tap a mantle source region.

The metavolcanic rocks lie stratigraphically beneath the Tshinakin Limestone and above the metasedimentary package (EBGs), and may characterize a metallogenically significant Late Proterozoic to Cambrian rifting event. Metasedimentary rock packages associated with unit EBG rocks east of Adams Lake host sedimentary exhalative-type massive-sulphide deposits (Höy, 1999).

The similar trends in the multielement plots and and spatial relationships of units EBFmv, EBFfv, and EBFin also suggest that these rocks represent a differentiation series. Bomb-sizes fragments of felsic composition are found within an intermediate matrix near the top of unit EBFin, which seems to represent the transition to dominantly felsic volcanic activity. We suggest that the Upper Devonian ($360 \pm 6$ Ma) age of unit EBFfv constrains the upper age of unit EBF.

Enrichment in $TiO_2$ and high Nb/Y ratios indicate an alkalic character for unit EBF. Also, enrichments in highly incompatible elements are likely the result of the interaction of melt with continental crust, either as a direct result of melting of continental crust or from contamination of a mantle-derived melt. The presence of an Upper Proterozoic zircon xenocryst from the Devonian meta-igneous rocks is further evidence of crustal contamination.

Alkalic bimodal volcanic rocks commonly occur in continental rift settings (Christiansen and Keith, 1996). Because of the bimodal alkalic nature of volcanism and penecontemporaneous deposition of a turbidite sequence, we interpret Devonian metavolcanic rocks of the Eagle Bay Assemblage to represent deposition in a rifted continental margin setting. The generation of Late Devonian meta-igneous rocks may be attributable to a rifting stage related to the development of the Slide Mountain ocean basin. Alternatively, magmatism may represent the vestiges of a failed rift.

Höy and Gouthier (1986) recognized the within-plate character of metabasic rocks associated with the Samatosum and Rea deposits. They interpreted the sequence of rocks that host the Homestake massive-sulphide–barite deposit to be of calc-alkaline arc affinity and the entire sequence as a rifted volcanic arc. However, this interpretation was based on the interpretation of an incomplete suite of elements, and we have submitted samples from the Homestake deposit for a more complete analysis. Structurally

these rocks appear to be fold repetitions of the metavolcanic units in the stratigraphic footwall to the Samatosum and Rea deposits. Therefore it is crucial to test whether these rocks are part of the same volcanic event or have an entirely different origin.

## CONCLUSIONS

Lower Cambrian unit EBG rocks are subalkaline and have rare-earth-element patterns that suggest derivation from a depleted-mantle source region. These rocks are associated with SEDEX-type massive-sulphide deposits on the Adams Plateau, and may have exploration potential in the Johnson and Adams lakes area.

Devonian bimodal metavolcanic rocks of the Eagle Bay Assemblage in the Johnson and Adams lakes area are alkalic and host polymetallic massive-sulphide deposits. These volcanic rocks have been subjected to continental crustal contamination as a direct result of either crustal melting or assimilation of continental crustal material by a mantle-derived melt. The Devonian sequence analyzed so far shows a differentiation trend from mafic to felsic with felsic units being the youngest volcanic units in the map area. It is apparent that the alkalic nature of the volcanism may be related to the precious-metal-enriched character of massive-sulphide deposits e.g. (Rea, Homestake) and records Devonian extensional tectonics operating along the western margin of North America.

## ACKNOWLEDGMENTS

Many thanks are offered to the following people: Jim and Barb Lewko for their hospitality at Johnson Lake Resort and Paul Schiarizza, Trygve Höy, George Simandl, Victor Preto, Bob Friesen (Teck Corporation), Ken Daughtry, and Andy Okulitch, for field visits and geological discussions. At the Pacific Geoscience Centre, Claudia Saheb, Richard Franklin, Roger Macleod, and Parm Dhesi are thanked for GIS assistance. Jennifer Porter and Morgan Soley provided excellent field assistance.

## REFERENCES

**Bailey, S.L., Paradis, S., and Johnston, S.T.**
2000: Geologic setting of the Devonian–Mississippian Rea and Samatosum VMS deposits of the Eagle Bay Assemblage, Adams Lake area, south-central British Columbia; *in* Geological Fieldwork 1999; British Columbia Ministry of Energy and Mines, Paper 2000-1, p. 287–296.

**Christiansen, E.H. and Keith, J.D.**
1996: Trace element systematics in silicic magmas: a metallogenic perspective; *in* Trace Element Geochemistry of Volcanic Rocks: Applications for Massive Sulphide Exploration, (ed.) D.A. Wyman; Geological Association of Canada, Short Course Notes, v. 12, p. 115–151.

**Dudas, F.O.**
1992: Petrogenetic evaluation of trace element discrimination diagrams; *in* Proceedings, International Conference On Basement Tectonics, v. 8, p. 93–127.

**Höy, T.**
1999: Massive sulphide deposits of the Eagle Bay Assemblage, Adams Plateau, south-central British Columbia (082M 3, 4); *in* Geological Fieldwork 1998; British Columbia Ministry of Energy and Mines, Paper 1999-1, p. 223–245.

**Höy, T. and Goutier, F.**
1986: Rea Gold (Hilton) and Homestake volcanogenic sulphide-barite deposits, southeastern British Columbia (82M/4W); *in* Geological Fieldwork 1985; British Columbia Ministry of Energy, Mines, and Petroleum Resources, Paper 1986-1.

**Irvine, T.N. and Baragar, W.R.A.**
1971: A guide to the chemical classification of the common volcanic rocks; Canadian Journal of Earth Sciences, v. 8, p. 523–548.

**Jenner, G.A.**
1996: Trace element geochemistry of igneous rocks: geochemical nomenclature and analytical geochemistry; *in* Trace Element Geochemistry of Volcanic Rocks: Applications for Massive Sulphide Exploration, (ed.) D.A. Wyman; Geological Association of Canada, Short Course Notes, v. 12, p. 51–77.

**Jenner, G.A., Longerich, H.P., Jackson, S.E., and Fryer, B.J.**
1990: ICP-MS a powerful tool for high precision trace-element analysis in earth sciences: evidence from selected U.S.G.S. reference samples; Chemical Geology, v. 83, p. 133–148.

**Lentz, D.R.**
1996: Trace-element systematics of felsic volcanic rocks associated with massive sulphide deposits in the Bathurst Mining Camp: petrogenetic, tectonic and chemostratigraphic implications for VHMS exploration; *in* Trace Element Geochemistry of Volcanic Rocks: Applications for Massive Sulphide Exploration, (ed.) D.A. Wyman; Geological Association of Canada, Short Course Notes, v. 12, p. 359–402.

**Longerich, H.P.**
1995: Analysis of pressed pellets of geological samples using wavelength-dispersive X-ray fluorescence spectrometry; X-Ray Spectrometry, v. 24.

**Meschede, P.M.**
1986: A method of discriminating between different types of mid-ocean ridge basalts and continental tholeiite with the Nb-Zr-Y diagram; Chemical Geology, v. 56, p. 207–218.

**Okulitch, A.V.**
1979: Lithology, stratigraphy, structure, and mineral occurrences of the Thompson–Shuswap–Okanagan area, British Columbia; Geological Survey of Canada, Open File 637.

**Pearce, J.A.**
1983: Role of the subcontinental lithosphere in magma genesis at active continental margins; *in* Continental Basalts and Mantle Xenoliths, (ed.) C.J. Hawkesworth and M.J. Norry; Shiva Publishing Limited, Nantwich, United Kingdom, p. 230–249.

**Pearce, J.A.** (cont.)
1996: A users guide to basalt discrimination diagrams; *in* Trace Element Geochemistry of Volcanic Rocks: Applications for Massive Sulphide Exploration, (ed.) D.A. Wyman; Geological Association of Canada, Short Course Notes, v. 12, p. 79–113.

**Pearce, J.A. and Cann, J.R.**
1973: Tectonic setting of basic volcanic rocks determined using trace element analyses; Earth and Planetary Science Letters, v. 19, p. 290–300.

**Pearce, J.A. and Norry, M.J.**
1979: Petrogenetic implications of Ti, Zr, Y, and Nb variations in volcanic rocks; Contributions to Mineralogy and Petrology, v. 69, p. 33–47.

**Pearce, J.A., Harris, N.B.W., and Tindle, A.G.**
1984: Trace element discrimination diagrams for the tectonic interpretation of granitic rocks; Journal of Petrology, v. 25, p. 956–983.

**Rollinson, H.**
1993: Using Geochemical Data; Evaluation, Presentation, Interpretation; Longman Group UK Ltd., London, United Kingdom, 352 p.

**Schiarizza, P. and Preto, V.A.**
1987: Geology of the Adams Plateau–Clearwater–Vavenby area; British Columbia Ministry of Energy, Mines, and Petroleum Resources, Paper 1987-1.

**Shervais, J.W.**
1982: Ti-V plots and the petrogenesis of modern and ophiolitic lavas; Earth and Planetary Science Letters, v. 59, p. 101–118.

**Sun, S. and McDonough, W.F.**
1989: Chemical and isotopic systematics of oceanic basalts: implications for mantle composition and processes; *in* Magmatism in the Ocean Basins, (ed.) A.D. Saunders and M.J. Norry; Geological Society Special Publication 42, p. 313–345.

**Swinden, H.S.**
1996: The application of volcanic geochemistry to the metallogeny of volcanic–hosted sulphide deposits in central Newfoundland; *in* Trace Element Geochemistry of Volcanic Rocks: Applications for Massive Sulphide Exploration, (ed.) D.A. Wyman; Geological Association of Canada, Short Course Notes, v. 12, p. 329–358.

**Wheeler, J.O. and McFeely, P.**
1991: Tectonic assemblage map of the Canadian Cordillera and adjacent parts of the United States of America; Geological Survey of Canada, Map 1712A, scale 1:2 000 000.

**Winchester, J.A. and Floyd, P.A**
1977: Geochemical discrimination of different magma series and their differentiation products using immobile elements; Chemical Geology, v. 20, p. 325–343.

**Wood, D.A.**
1980: The application of a Th-Hf-Ta diagram to problems of tectonomagmatic classification and to establishing the nature of crustal contamination of basaltic lavas of the British Tertiary volcanic province; Earth and Planetary Science Letters, v. 50, p. 11–30.

Geological Survey of Canada Project 990002

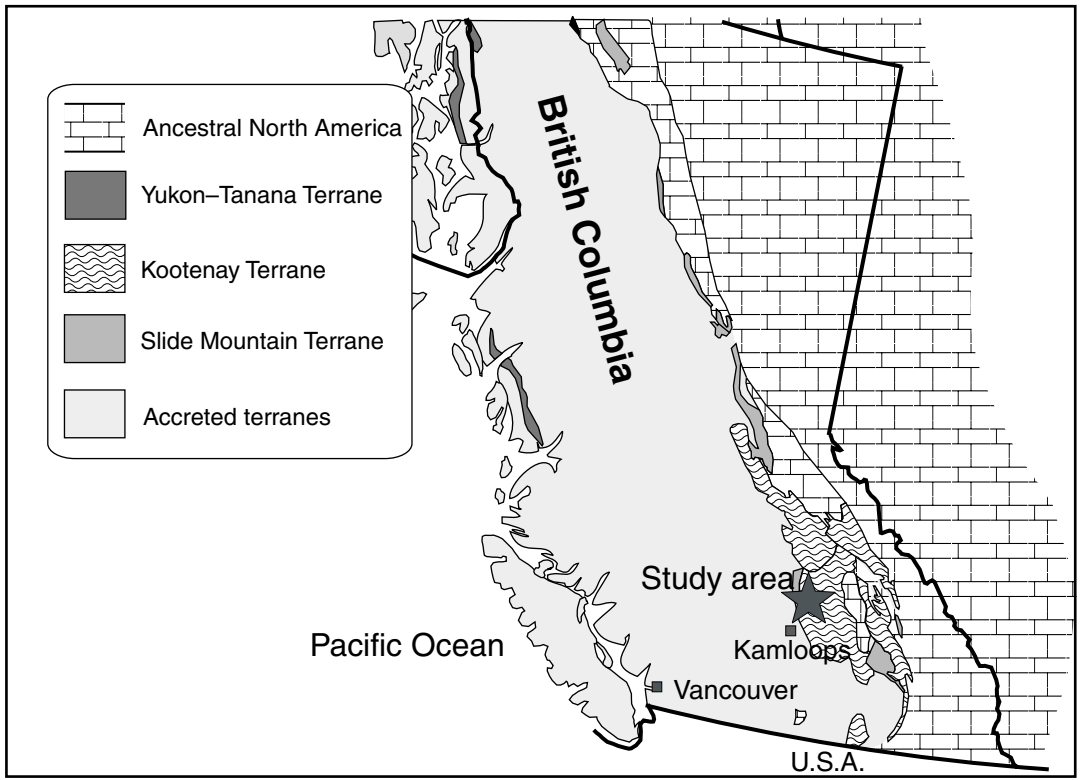


**Figure 1.** Location of the study area within the Kootenay Terrane of south-central British Columbia (*modified from* Wheeler and McFeely, 1991).

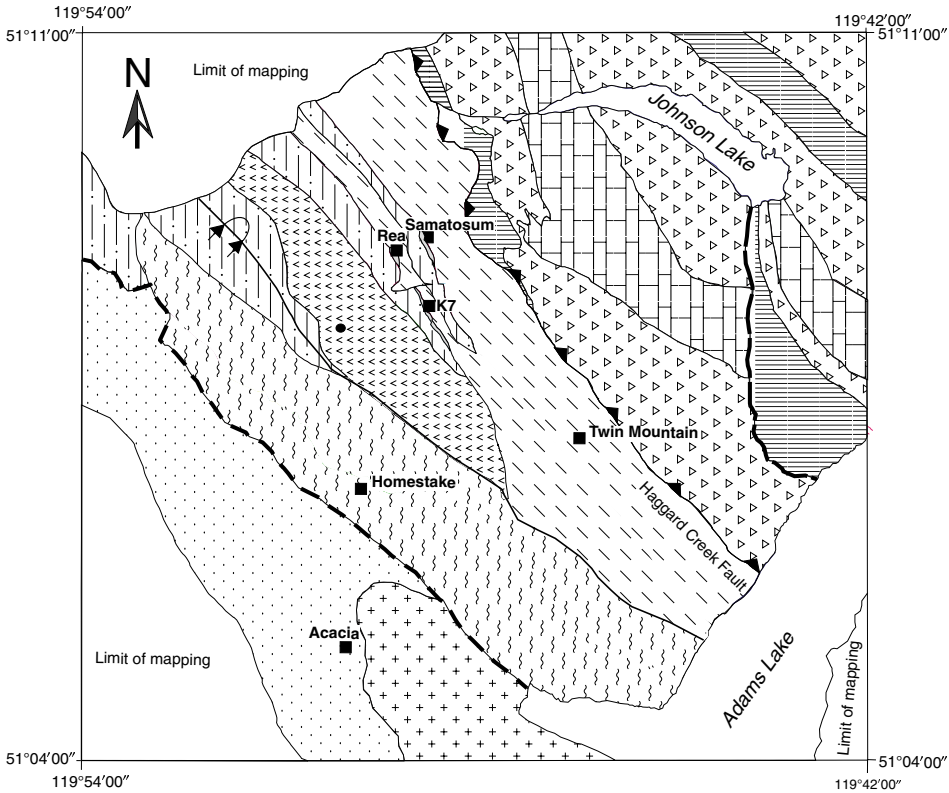


## LEGEND

| | | |
|---|---|---|
| | EBFfv | Felsic metavolcanic rocks: Quartz-sericite schist derived from quartz-feldspar-phyric rhyolite, and quartz-feldspar crystal lithic tuff, lapilli, to bomb-sized pyroclastics. |
| | EBFin | Mafic to intermediate metavolcanic rocks: Chlorite schist derived from agglomerate and pyroclastics, dominantly tuffs, locally up to 80% fragments of felsic composition. |
| | EBS | Metasedimentary rocks: Dominantly fine- to coarse-grained quartzite, quartz-pebble lithic conglomerate, minor phyllite, quartz-sericite-ankerite schist, chlorite schist, and marble. |
| | EBF/EBP | Metasedimentary rocks: Phyllite, and quartz-sericite schist derived from argillite to quartz wacke, sandstone, and pebble conglomerate. |
| | | Alteration zone: (Rea and Samatosum horizons) sericite-quartz-carbonate-pyrite alteration of metasedimentary rocks |
| | EBFmv | Mafic metavolcanic flows and volcaniclastic rocks: Calcareous chlorite schist derived from mafic volcanic rocks; mafic lapilli tuffs, pillow lavas, and pillow breccias, massive flows and minor diorite sills present |
| | Dgn | Devonian orthoschist, quartz-feldspar-sericite-ankerite schist derived from foliated granodiorite to diorite |
| | EBG | Mafic metavolcanic rocks: Light green, calcareous chlorite schist and greenstone derived from pillows, pillow breccias, and feldspathic crystal tuffs, abundant epidote alteration |
| | EBGt | Tshinakin Limestone: Buff-white-weathering, layered, finely crystalline, white to grey marble and dolostone |
| | EBGs | Metasedimentary rocks: Phyllite derived from shale and siltstone, banded chert plus minor white-grey marble units |

Devonian U-Pb zircon date
Mineral occurrence
Fault (undefined)
Overturned syncline
Thrust fault

**Figure 2.** Simplified geology of the Johnson and Adams lakes area (this study).

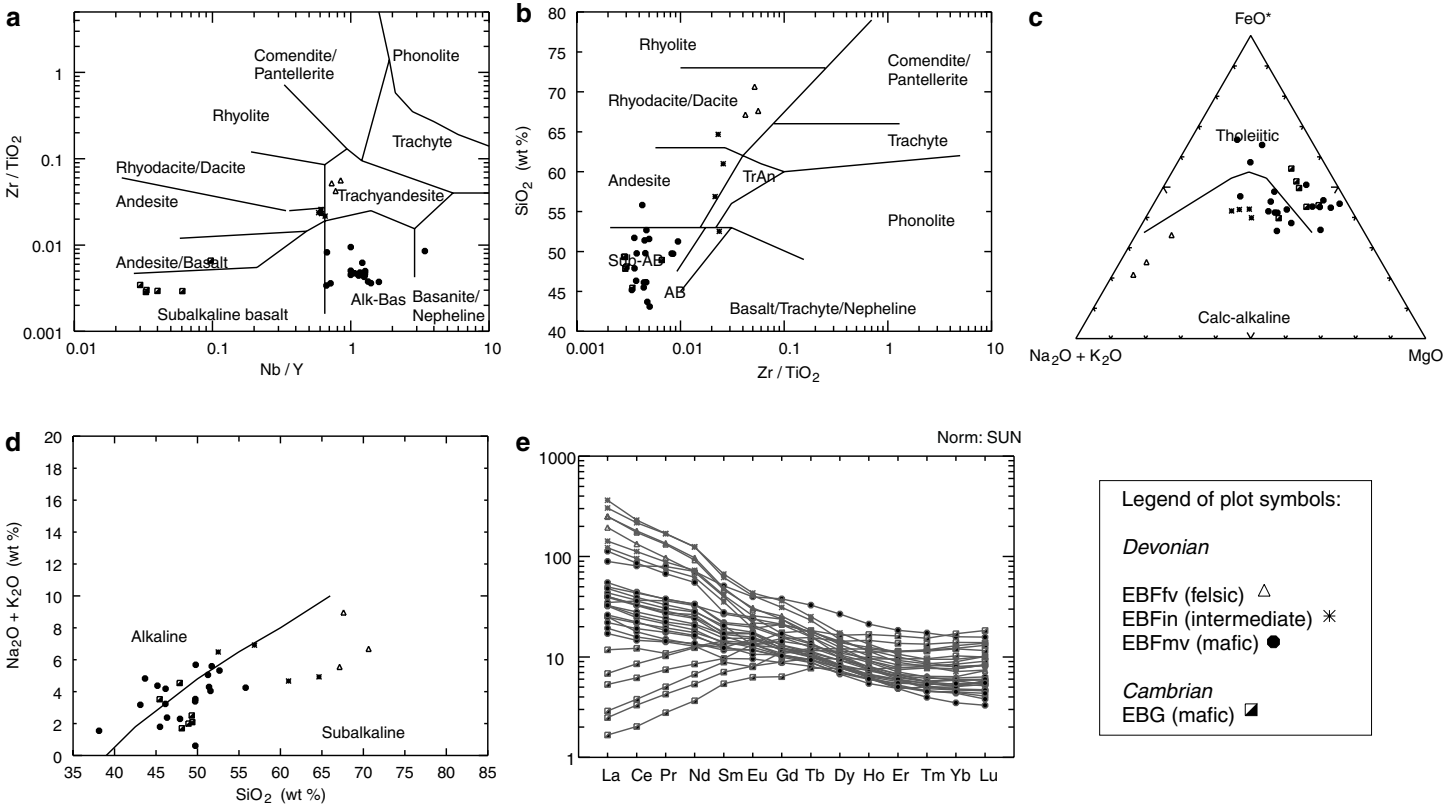


**Figure 3.** Discrimination diagrams for basalts. **a)** Winchester and Floyd (1977) Zr-$TiO_2$–Nb/Y diagram; unit EBG has a subalkalic signature, unit EBFmv has an alkalic signature. **b)** Plot of $SiO_2$-$Zr/TiO_2$ *after* Winchester and Floyd (1977). **c)** Irvine and Baragar (1971) AFM diagram; the addition of alkalis due to sericite alteration makes major-element discrimination suspect. **d)** Alkali vs. $SiO_2$ discrimination diagram (*after* Irvine and Baragar, 1971). **e)** Chondrite (SUN)-normalized rare-earth-element plot of samples from this study; note the relative enrichments and depletions in the REEs.

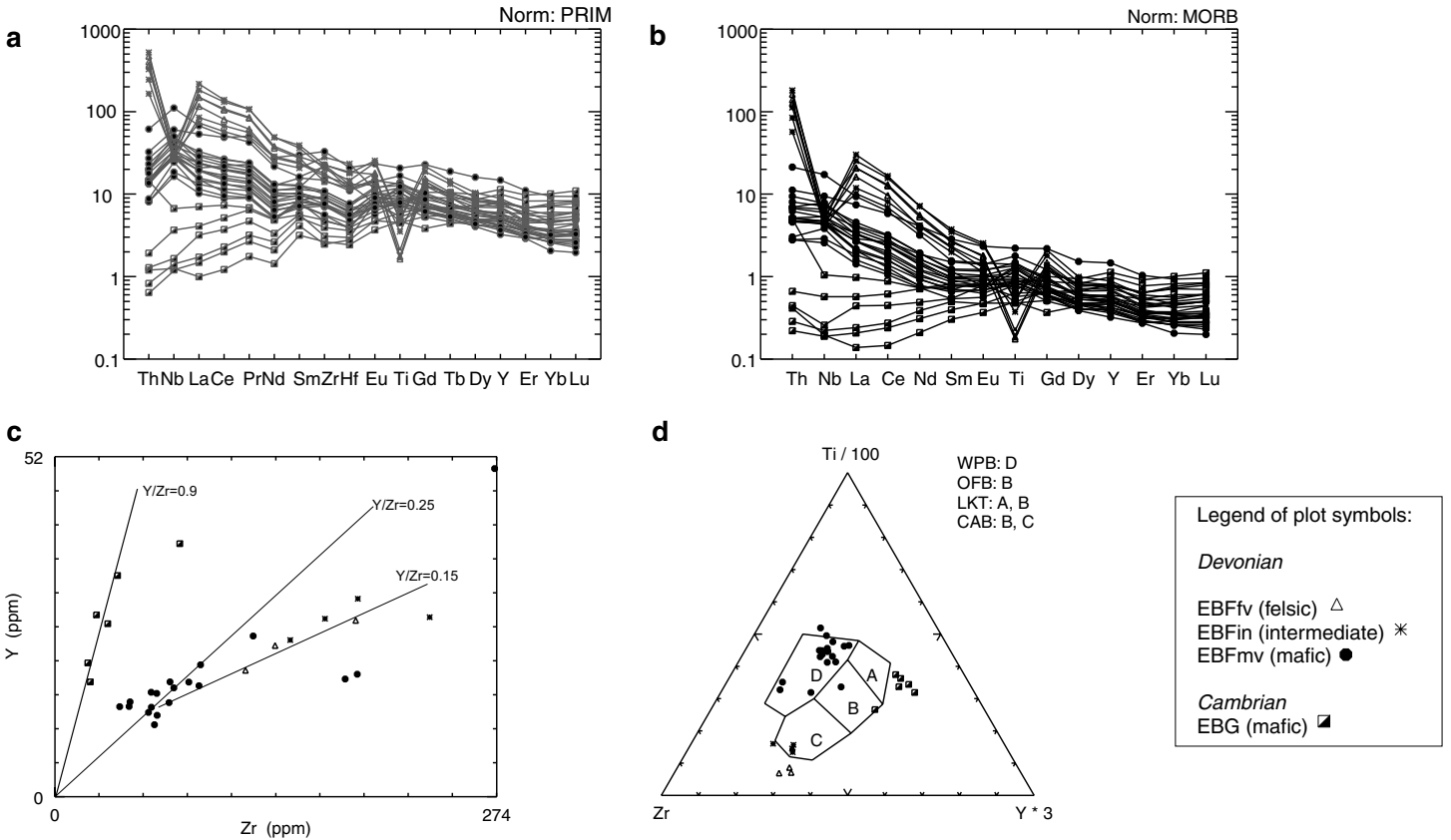


**Figure 4. a)** Primitive-mantle-normalized multielement plot; note the apparent negative anomalies of Nb and Ti in units EBFfv and EBFin compared with the slight positive anomalies in unit EBFmv. **b)** Mid-ocean-ridge basalt (MORB) normalized multielement plot; the flat pattern of the Cambrian metavolcanic rocks suggest a depleted-mantle source region. **c)** Yttrium/zirconium ratio; note the differentiation trend in the alkalic suite. **d)** Pearce and Cann's (1973) tectonic discrimination diagram.

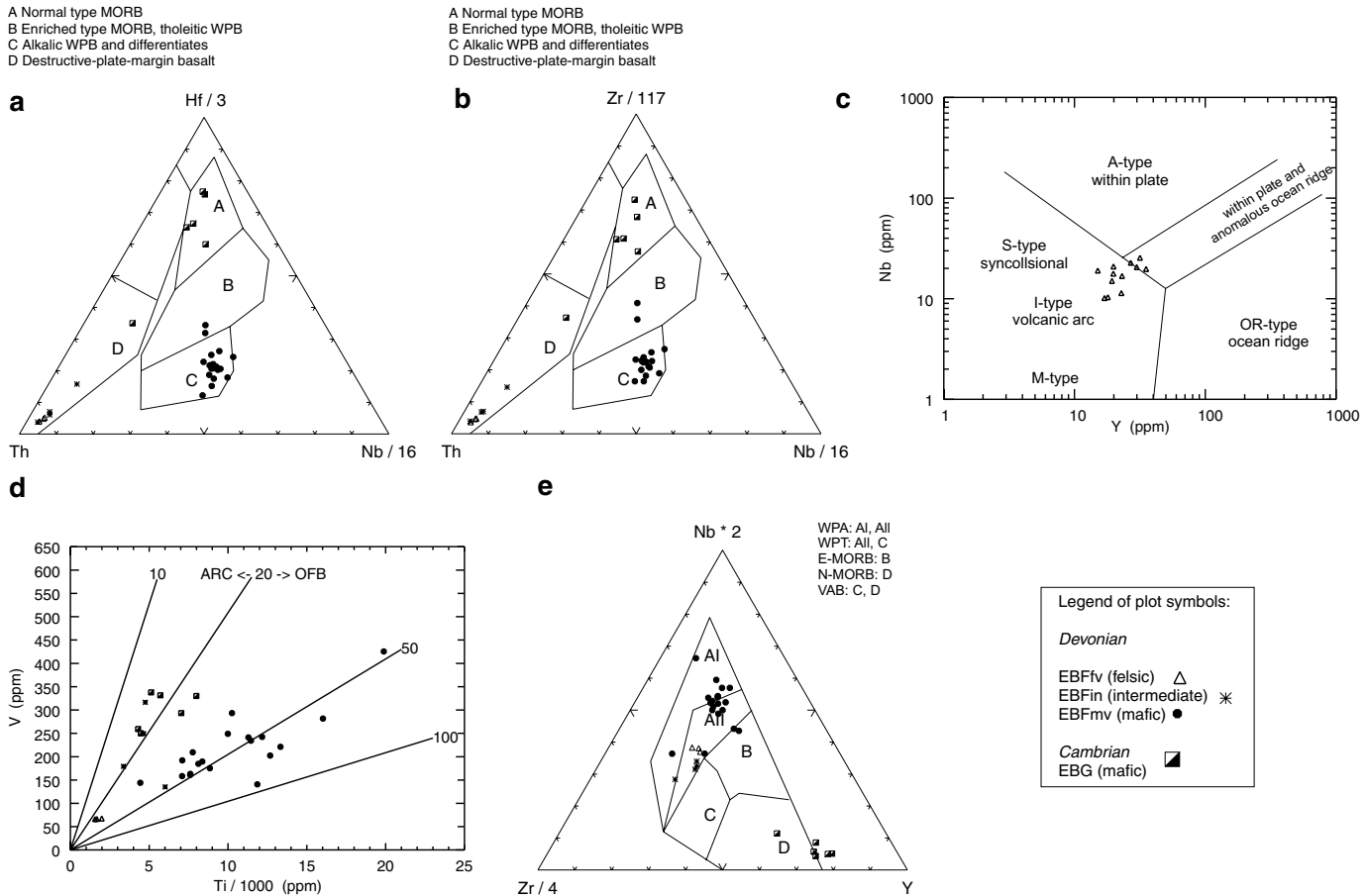


**Figure 5.** Trace-element tectonic discrimination diagrams; the legend shows precursor symbols. **a), b)** Basalt discrimination diagrams of Wood (1980); unit EBFmv shows a within-plate basalt character, unit EBG rocks plot in the N-MORB field. **c)** Niobium/yttrium felsic discrimination diagram of Pearce et al. (1984). **d)** Unit EBFmv shows low V/Ti ratios, whereas unit EBG shows higher ratios, similar to mid-ocean-ridge basalts (*after* Shervais, 1982). **e)** Meschede's (1986) Nb-Y-Zr discrimination diagram; unit EBFmv shows a within-plate basalt character; unit EBG shows characteristics of N-MORB.

**Table 1a.** Results of major- and trace-element analyses on volcanic rocks from the Johnson and Adams lakes area, Eagle Bay Assemblage.

| UNIT | EBFmv | EBFmv | EBFmv | EBFmv | EBFmv | EBFmv | EBFmv | EBFmv |
|---|---|---|---|---|---|---|---|---|
| Sample Name | SLB99-98B | SLB99-6A | SLB99-35 | SLB99-59 | SLB99-54 | SLB99-138D | SLB99-6B | SLB99-106 |
| $SiO_2$ | 49.80 | 52.67 | 43.69 | 45.19 | 49.75 | 38.13 | 46.14 | 51.72 |
| $TiO_2$ | 2.67 | 1.27 | 1.48 | 1.18 | 3.32 | 0.74 | 2.03 | 1.30 |
| $Al_2O_3$ | 16.39 | 11.73 | 13.20 | 11.38 | 13.64 | 6.43 | 14.46 | 17.31 |
| $Fe_2O_3$ | 18.14 | 1.60 | 1.08 | 1.84 | 1.31 | 1.40 | 2.02 | 2.07 |
| FeO | 1.43 | 6.18 | 6.72 | 7.47 | 14.07 | 10.90 | 11.48 | 7.98 |
| MnO | 0.05 | 0.16 | 0.19 | 0.15 | 0.73 | 0.49 | 0.17 | 0.16 |
| MgO | 3.60 | 8.52 | 3.85 | 6.68 | 5.07 | 14.40 | 14.00 | 7.97 |
| CaO | 1.90 | 12.36 | 24.70 | 21.59 | 7.83 | 25.79 | 6.18 | 5.76 |
| $Na_2O$ | 0.10 | 5.22 | 4.44 | 4.25 | 3.49 | 0.56 | 3.08 | 4.77 |
| $K_2O$ | 5.58 | 0.10 | 0.38 | 0.13 | 0.04 | 0.99 | 0.15 | 0.83 |
| $P_2O_5$ | 0.34 | 0.19 | 0.25 | 0.13 | 0.74 | 0.18 | 0.30 | 0.13 |
| LOI | 0.00 | 0.00 | 12.80 | 10.20 | 0.00 | 27.30 | 0.00 | 0.00 |
| Cr | 780 | 405 | 211 | 578 | 41 | 263 | 768 | 420 |
| Ni | 531 | 188 | 66 | 336 | 38 | 177 | 411 | 103 |
| Co | 36 | 33 | 28 | 51 | 36 | 32 | 67 | 45 |
| Sc | 36 | 20 | 23 | 23 | 35 | 14 | 26 | 34 |
| V | 282 | 161 | 175 | 192 | 425 | 144 | 242 | 209 |
| Cu | 98 | 126 | 76 | 46 | 257 | 52 | 104 | 80 |
| Pb | 2 | 4 | 0 | 0 | 4 | 3 | 0 | 0 |
| Zn | 81 | 54 | 61 | 79 | 159 | 56 | 109 | 86 |
| Bi | 0.00 | 0.00 | 0.36 | 0.00 | 0.00 | 0.00 | 0.21 | 0.00 |
| Cd | 0.00 | 0.00 | 0.00 | 0.00 | 0.00 | 0.00 | 0.00 | 0.00 |
| In | 0.08 | 0.00 | 0.00 | 0.06 | 0.13 | 0.00 | 0.06 | 0.05 |
| Sn | 1.33 | 0.64 | 0.96 | 1.38 | 2.29 | 0.00 | 1.49 | 0.73 |
| Mo | 0.20 | 0.53 | 0.36 | 0.23 | 0.76 | 0.42 | 0.00 | 0.00 |
| Sb | 0.61 | 0.75 | 0.36 | 0.34 | 0.00 | 0.42 | 0.64 | 0.41 |
| Ag | 0.0 | 0.0 | 0.0 | 0.0 | 0.0 | 0.1 | 0.0 | 0.1 |
| Rb | 143 | 1 | 6 | 1 | 1 | 27 | 3 | 10 |
| Cs | 4.51 | 0.11 | 0.22 | 0.07 | 0.15 | 0.67 | 0.16 | 0.32 |
| Ba | 1639 | 203 | 116 | 218 | 49 | 335 | 117 | 404 |
| Sr | 20 | 220 | 491 | 240 | 317 | 277 | 120 | 306 |
| Tl | 0.45 | 0.00 | 0.04 | 0.00 | 0.00 | 0.47 | 0.00 | 0.02 |
| Ga | 24 | 9 | 14 | 11 | 25 | 8 | 21 | 17 |
| Ta | 1.64 | 0.79 | 0.83 | 0.44 | 1.85 | 0.77 | 1.28 | 0.53 |
| Nb | 27.7 | 17.1 | 16.8 | 9.2 | 33.8 | 16.8 | 25.5 | 10.4 |
| Hf | 3.07 | 1.49 | 1.68 | 1.09 | 5.89 | 1.08 | 2.13 | 1.24 |
| Zr | 123 | 60 | 71 | 40 | 273 | 46 | 90 | 47 |
| Y | 25 | 16 | 14 | 14 | 50 | 14 | 20 | 15 |
| Th | 1.74 | 0.88 | 0.96 | 0.52 | 2.07 | 0.95 | 1.49 | 0.52 |
| U | 0.47 | 0.21 | 0.32 | 0.22 | 0.65 | 0.27 | 0.32 | 0.15 |
| La | 14.34 | 10.56 | 13.20 | 5.63 | 29.46 | 8.24 | 18.07 | 7.26 |
| Ce | 31.76 | 21.32 | 28.81 | 12.65 | 69.82 | 15.37 | 38.27 | 16.58 |
| Pr | 4.71 | 2.77 | 3.72 | 1.84 | 10.36 | 1.96 | 4.89 | 2.28 |
| Nd | 20.49 | 11.73 | 15.60 | 8.05 | 44.73 | 8.38 | 21.26 | 10.05 |
| Sm | 5.43 | 2.77 | 3.60 | 1.95 | 10.36 | 2.51 | 4.46 | 2.59 |
| Eu | 1.84 | 1.03 | 1.32 | 0.74 | 3.05 | 1.16 | 1.59 | 0.82 |
| Gd | 5.84 | 2.88 | 3.60 | 2.41 | 10.47 | 3.21 | 4.46 | 2.90 |
| Tb | 0.89 | 0.47 | 0.54 | 0.40 | 1.64 | 0.50 | 0.67 | 0.47 |
| Dy | 4.92 | 2.67 | 2.88 | 2.41 | 9.16 | 2.79 | 3.61 | 2.69 |
| Ho | 0.90 | 0.49 | 0.52 | 0.47 | 1.64 | 0.47 | 0.68 | 0.52 |
| Er | 2.25 | 1.28 | 1.32 | 1.15 | 4.15 | 1.09 | 1.59 | 1.35 |
| Tm | 0.31 | 0.18 | 0.19 | 0.16 | 0.61 | 0.14 | 0.22 | 0.18 |
| Yb | 1.74 | 1.06 | 1.14 | 0.98 | 3.49 | 0.77 | 1.28 | 1.04 |
| Lu | 0.28 | 0.16 | 0.19 | 0.14 | 0.53 | 0.11 | 0.18 | 0.16 |
| Be | 1.23 | 0.85 | 0.00 | 0.00 | 1.96 | 0.00 | 0.53 | 0.52 |
| $Zr/TiO_2$ | 45.98 | 47.06 | 47.97 | 33.98 | 82.24 | 62.26 | 44.50 | 36.00 |
| Zr/Hf | 40.00 | 40.00 | 42.14 | 36.84 | 46.30 | 42.86 | 42.50 | 37.50 |
| Y/Zr | 0.20 | 0.27 | 0.20 | 0.34 | 0.18 | 0.30 | 0.22 | 0.31 |
| Nb/Y | 1.12 | 1.07 | 1.17 | 0.67 | 0.67 | 1.21 | 1.26 | 0.71 |

**Table 1a.** (cont.)

| UNIT | EBFmv | EBFmv | EBFmv | EBFmn | EBG | EBFmv | EBG | EBFmv |
|---|---|---|---|---|---|---|---|---|
| Sample Name | SLB99-166B | SLB99-193 | SLB99-166C | SLB99-45 | SLB99-39 | SLB99-101 | SLB99-09 | SLB99-42 |
| $SiO_2$ | 46.33 | 46.16 | 51.40 | 49.76 | 48.11 | 47.89 | 47.85 | 45.49 |
| $TiO_2$ | 2.22 | 1.91 | 1.40 | 1.89 | 0.86 | 1.71 | 0.75 | 1.67 |
| $Al_2O_3$ | 13.46 | 15.95 | 13.85 | 13.58 | 16.79 | 16.77 | 17.23 | 14.53 |
| $Fe_2O_3$ | 2.34 | 1.47 | 2.43 | 1.87 | 2.88 | 7.17 | 2.74 | 1.31 |
| FeO | 9.95 | 9.39 | 6.08 | 10.19 | 6.18 | 6.84 | 5.71 | 11.67 |
| MnO | 0.21 | 0.15 | 0.22 | 0.22 | 0.14 | 0.09 | 0.18 | 0.17 |
| MgO | 13.31 | 7.17 | 7.33 | 14.17 | 9.44 | 10.60 | 7.84 | 13.48 |
| CaO | 9.52 | 13.34 | 12.78 | 7.47 | 13.84 | 6.40 | 13.11 | 9.67 |
| $Na_2O$ | 2.34 | 3.05 | 1.46 | 0.23 | 1.55 | 0.11 | 3.07 | 1.19 |
| $K_2O$ | 0.04 | 1.13 | 2.84 | 0.39 | 0.16 | 2.18 | 1.47 | 0.61 |
| $P_2O_5$ | 0.28 | 0.26 | 0.21 | 0.23 | 0.05 | 0.22 | 0.05 | 0.21 |
| LOI | 14.50 | 0.00 | 16.50 | 0.00 | 0.00 | 0.00 | 0.00 | 15.10 |
| Cr | 574 | 256 | 203 | 506 | 512 | 959 | 464 | 713 |
| Ni | 342 | 83 | 83 | 327 | 167 | 433 | 150 | 387 |
| Co | 71 | 35 | 32 | 52 | 41 | 77 | 44 | 80 |
| Sc | 26 | 27 | 24 | 30 | 43 | 40 | 38 | 29 |
| V | 221 | 234 | 190 | 241 | 338 | 294 | 250 | 249 |
| Cu | 66 | 153 | 69 | 84 | 69 | 0 | 174 | 127 |
| Pb | 6 | 0 | 5 | 9 | 0 | 0 | 0 | 2 |
| Zn | 122 | 92 | 51 | 226 | 54 | 130 | 64 | 123 |
| Bi | 0.00 | 0.00 | 0.00 | 0.00 | 0.00 | 0.00 | 0.00 | 0.00 |
| Cd | 0.00 | 0.00 | 0.00 | 0.00 | 0.00 | 0.00 | 0.00 | 0.00 |
| In | 0.00 | 0.08 | 0.00 | 0.00 | 0.09 | 0.08 | 0.00 | 0.06 |
| Sn | 1.40 | 1.24 | 0.00 | 1.40 | 0.72 | 0.99 | 0.00 | 0.83 |
| Mo | 0.00 | 0.00 | 0.00 | 0.00 | 0.00 | 0.00 | 0.00 | 0.36 |
| Sb | 0.70 | 0.00 | 0.24 | 1.29 | 0.52 | 0.88 | 0.22 | 1.31 |
| Ag | 0.0 | 0.1 | 0.0 | 0.0 | 0.0 | 0.0 | 0.0 | 0.0 |
| Rb | 0 | 23 | 62 | 12 | 3 | 46 | 25 | 15 |
| Cs | 0.06 | 0.87 | 1.94 | 0.29 | 0.11 | 1.99 | 1.87 | 0.31 |
| Ba | 49 | 317 | 948 | 363 | 80 | 386 | 340 | 703 |
| Sr | 102 | 210 | 115 | 177 | 77 | 92 | 43 | 132 |
| Tl | 0.00 | 0.17 | 0.72 | 0.26 | 0.00 | 0.13 | 0.10 | 0.12 |
| Ga | 16 | 19 | 16 | 18 | 24 | 18 | 13 | 18 |
| Ta | 1.52 | 1.12 | 0.77 | 1.40 | 0.07 | 0.71 | 0.05 | 0.98 |
| Nb | 28.1 | 21.5 | 15.8 | 23.4 | 0.9 | 15.4 | 0.7 | 19.1 |
| Hf | 1.99 | 2.15 | 1.46 | 1.76 | 0.83 | 1.43 | 0.68 | 1.67 |
| Zr | 83 | 89 | 63 | 71 | 26 | 62 | 22 | 74 |
| Y | 18 | 17 | 16 | 18 | 28 | 11 | 18 | 17 |
| Th | 1.29 | 1.24 | 0.86 | 1.29 | 0.08 | 0.87 | 0.08 | 0.95 |
| U | 0.34 | 0.37 | 0.24 | 0.36 | 0.04 | 0.25 | 0.08 | 0.25 |
| La | 16.38 | 15.84 | 10.69 | 12.88 | 1.75 | 8.17 | 0.55 | 13.10 |
| Ce | 37.44 | 33.94 | 24.30 | 28.10 | 5.36 | 18.76 | 1.76 | 28.58 |
| Pr | 4.91 | 4.30 | 3.16 | 3.51 | 0.97 | 2.54 | 0.36 | 3.57 |
| Nd | 21.06 | 18.10 | 13.37 | 15.22 | 5.36 | 11.04 | 2.30 | 16.67 |
| Sm | 4.33 | 3.96 | 3.40 | 3.28 | 1.96 | 2.87 | 1.10 | 3.45 |
| Eu | 1.52 | 1.36 | 1.22 | 1.01 | 1.03 | 0.96 | 0.48 | 1.31 |
| Gd | 4.33 | 3.62 | 3.40 | 3.40 | 2.99 | 2.87 | 1.76 | 3.33 |
| Tb | 0.62 | 0.57 | 0.51 | 0.55 | 0.58 | 0.44 | 0.38 | 0.52 |
| Dy | 3.39 | 3.17 | 2.79 | 3.16 | 3.91 | 2.32 | 2.63 | 2.86 |
| Ho | 0.61 | 0.58 | 0.50 | 0.62 | 0.86 | 0.42 | 0.58 | 0.56 |
| Er | 1.40 | 1.47 | 1.34 | 1.52 | 2.58 | 1.09 | 1.76 | 1.43 |
| Tm | 0.20 | 0.21 | 0.17 | 0.20 | 0.41 | 0.18 | 0.29 | 0.20 |
| Yb | 1.17 | 1.36 | 1.03 | 1.29 | 2.68 | 1.10 | 1.87 | 1.31 |
| Lu | 0.18 | 0.21 | 0.16 | 0.20 | 0.44 | 0.20 | 0.31 | 0.20 |
| Be | 0.00 | 0.00 | 0.00 | 0.00 | 0.00 | 0.66 | 0.00 | 0.60 |
| $Zr/TiO_2$ | 37.37 | 46.75 | 45.22 | 37.89 | 30.12 | 36.13 | 29.41 | 44.29 |
| Zr/Hf | 41.76 | 41.58 | 43.33 | 40.67 | 30.86 | 43.08 | 32.26 | 44.29 |
| Y/Zr | 0.21 | 0.19 | 0.25 | 0.25 | 1.08 | 0.18 | 0.80 | 0.23 |
| Nb/Y | 1.60 | 1.27 | 1.00 | 1.33 | 0.03 | 1.40 | 0.04 | 1.14 |

**Table 1b.** Results of major- and trace-element analyses on volcanic rocks from the Johnson and Adams lakes area, Eagle Bay Assemblage.

| UNIT | EBG | EBG | EBFmv | EBFmv | EBFmv | EBG | EBFmv | EBG |
|---|---|---|---|---|---|---|---|---|
| Sample Name | SLB99-67C | SLB99-48 | SLB99-81 | SLB99-107B | SLB99-05 | SLB99-17B | SLB99-22C | SLB99-17C |
| $SiO_2$ | 48.93 | 49.31 | 49.73 | 51.27 | 55.81 | 49.37 | 43.12 | 45.44 |
| $TiO_2$ | 1.17 | 1.33 | 2.12 | 1.98 | 1.35 | 0.72 | 1.18 | 0.95 |
| $Al_2O_3$ | 12.32 | 14.97 | 14.51 | 15.84 | 10.86 | 16.59 | 11.46 | 19.17 |
| $Fe_2O_3$ | 0.47 | 3.69 | 1.69 | 12.92 | 2.15 | 4.92 | 1.00 | 1.69 |
| FeO | 10.44 | 7.69 | 8.55 | 2.40 | 6.45 | 5.43 | 6.48 | 10.91 |
| MnO | 0.40 | 0.21 | 0.24 | 0.09 | 0.14 | 0.16 | 0.21 | 0.26 |
| MgO | 6.49 | 8.63 | 14.57 | 5.00 | 9.35 | 7.05 | 6.74 | 12.62 |
| CaO | 17.62 | 11.55 | 4.56 | 4.97 | 9.44 | 13.63 | 26.48 | 5.36 |
| $Na_2O$ | 1.76 | 2.46 | 3.38 | 3.33 | 3.55 | 2.05 | 2.87 | 2.75 |
| $K_2O$ | 0.25 | 0.05 | 0.02 | 1.72 | 0.70 | 0.04 | 0.31 | 0.77 |
| $P_2O_5$ | 0.15 | 0.11 | 0.64 | 0.48 | 0.19 | 0.04 | 0.15 | 0.05 |
| LOI | 12.30 | 0.00 | 0.00 | 0.00 | 0.00 | 0.00 | 14.40 | 0.00 |
| Cr | 150 | 321 | 489 | 447 | 476 | 491 | 501 | 627 |
| Ni | 59 | 69 | 240 | 438 | 259 | 159 | 222 | 244 |
| Co | 41 | 32 | 50 | 63 | 54 | 49 | 44 | 64 |
| Sc | 33 | 47 | 24 | 32 | 19 | 43 | 21 | 56 |
| V | 293 | 330 | 203 | 141 | 185 | 259 | 158 | 332 |
| Cu | 92 | 52 | 64 | 0 | 109 | 15 | 41 | 72 |
| Pb | 5 | 0 | 2 | 0 | 3 | 4 | 2 | 0 |
| Zn | 92 | 88 | 78 | 89 | 63 | 60 | 54 | 91 |
| Bi | 0.35 | 0.00 | 0.00 | 0.00 | 0.00 | 0.00 | 0.00 | 0.00 |
| Cd | 0.35 | 0.00 | 0.00 | 0.00 | 0.00 | 0.00 | 0.00 | 0.00 |
| In | 0.11 | 0.07 | 0.07 | 0.05 | 0.08 | 0.00 | 0.09 | 0.06 |
| Sn | 0.94 | 0.62 | 1.24 | 1.35 | 1.83 | 0.61 | 1.00 | 0.64 |
| Mo | 0.35 | 0.00 | 0.00 | 0.00 | 0.43 | 0.00 | 0.00 | 0.00 |
| Sb | 0.23 | 0.41 | 0.56 | 0.00 | 0.32 | 0.92 | 1.00 | 0.00 |
| Ag | 0.0 | 0.1 | 0.0 | 0.0 | 0.0 | 0.0 | 0.0 | 0.0 |
| Rb | 7 | 2 | 0 | 33 | 22 | 0 | 6 | 18 |
| Cs | 0.21 | 0.11 | 0.05 | 0.94 | 5.59 | 0.05 | 0.22 | 0.65 |
| Ba | 61 | 47 | 24 | 333 | 215 | 68 | 274 | 254 |
| Sr | 304 | 45 | 115 | 144 | 206 | 249 | 523 | 81 |
| Tl | 0.04 | 0.00 | 0.00 | 0.09 | 0.12 | 0.00 | 0.02 | 0.10 |
| Ga | 15 | 17 | 19 | 15 | 11 | 14 | 11 | 19 |
| Ta | 0.23 | 0.15 | 2.93 | 1.04 | 0.86 | 0.05 | 0.64 | 0.07 |
| Nb | 3.8 | 2.1 | 61.9 | 18.8 | 16.1 | 0.7 | 13.7 | 0.8 |
| Hf | 1.88 | 1.13 | 3.26 | 3.65 | 1.51 | 0.78 | 1.37 | 1.01 |
| Zr | 77 | 39 | 180 | 188 | 58 | 20 | 60 | 33 |
| Y | 39 | 34 | 18 | 19 | 13 | 20 | 14 | 26 |
| Th | 0.93 | 0.12 | 3.94 | 1.15 | 0.85 | 0.04 | 0.56 | 0.05 |
| U | 0.59 | 0.04 | 0.98 | 0.21 | 0.22 | 0.02 | 0.25 | 0.00 |
| La | 3.87 | 2.26 | 37.13 | 11.46 | 10.75 | 0.82 | 6.36 | 0.95 |
| Ce | 10.56 | 7.38 | 74.26 | 31.26 | 22.58 | 2.87 | 13.71 | 3.28 |
| Pr | 1.41 | 1.33 | 8.78 | 3.96 | 2.90 | 0.55 | 1.87 | 0.66 |
| Nd | 7.98 | 7.79 | 34.88 | 17.71 | 12.90 | 3.38 | 8.60 | 4.24 |
| Sm | 2.93 | 2.77 | 5.63 | 4.17 | 3.12 | 1.43 | 2.37 | 1.80 |
| Eu | 1.06 | 1.03 | 1.91 | 1.01 | 1.18 | 0.62 | 0.91 | 0.61 |
| Gd | 4.81 | 4.20 | 4.73 | 3.96 | 3.23 | 2.46 | 2.74 | 3.07 |
| Tb | 0.92 | 0.78 | 0.69 | 0.65 | 0.49 | 0.48 | 0.44 | 0.60 |
| Dy | 5.63 | 4.92 | 3.38 | 3.75 | 2.69 | 3.28 | 2.37 | 4.13 |
| Ho | 1.29 | 1.13 | 0.59 | 0.75 | 0.48 | 0.74 | 0.46 | 0.92 |
| Er | 3.64 | 3.08 | 1.35 | 1.88 | 1.18 | 2.15 | 1.23 | 2.54 |
| Tm | 0.54 | 0.47 | 0.19 | 0.29 | 0.16 | 0.34 | 0.19 | 0.40 |
| Yb | 3.75 | 3.08 | 1.11 | 1.77 | 0.96 | 2.25 | 1.20 | 2.65 |
| Lu | 0.62 | 0.47 | 0.18 | 0.28 | 0.13 | 0.34 | 0.19 | 0.39 |
| Be | 0.00 | 0.00 | 1.01 | 1.04 | 1.18 | 0.00 | 0.00 | 0.53 |
| $Zr/TiO_2$ | 66.00 | 29.23 | 85.11 | 94.74 | 42.86 | 28.57 | 50.53 | 34.44 |
| Zr/Hf | 41.25 | 34.55 | 55.17 | 51.43 | 38.57 | 26.32 | 43.64 | 32.63 |
| Y/Zr | 0.50 | 0.87 | 0.10 | 0.10 | 0.22 | 1.00 | 0.23 | 0.81 |
| Nb/Y | 0.10 | 0.06 | 3.44 | 1.00 | 1.25 | 0.03 | 1.00 | 0.03 |

**Table 1b.** (cont.)

| UNIT | EBFmv | EBFfv | EBFfv | EBFfv | EBFin | EBFin | EBFin | EBFin |
|---|---|---|---|---|---|---|---|---|
| Sample Name | SLB99-61 | SLB99-31 | SLB99-33 | SLB99-192B | SLB99-50 | SLB99-182 | SLB99-179 | SLB99-168 |
| $SiO_2$ | 51.57 | 70.63 | 67.61 | 67.15 | 64.67 | 56.88 | 52.52 | 60.99 |
| $TiO_2$ | 1.27 | 0.26 | 0.33 | 0.28 | 1.00 | 0.78 | 0.79 | 0.56 |
| $Al_2O_3$ | 12.24 | 13.66 | 16.59 | 13.86 | 14.37 | 18.44 | 20.15 | 16.37 |
| $Fe_2O_3$ | 1.59 | 1.16 | 2.07 | 1.29 | 0.74 | 2.30 | 3.86 | 2.29 |
| FeO | 6.12 | 1.47 | 0.73 | 2.26 | 5.92 | 6.39 | 6.06 | 4.17 |
| MnO | 0.14 | 0.05 | 0.05 | 0.09 | 0.12 | 0.09 | 0.11 | 0.11 |
| MgO | 6.55 | 0.76 | 0.73 | 1.03 | 4.99 | 4.71 | 6.30 | 3.72 |
| CaO | 16.34 | 5.16 | 2.67 | 8.27 | 3.10 | 2.95 | 3.25 | 6.67 |
| $Na_2O$ | 3.74 | 3.47 | 3.32 | 2.79 | 2.54 | 4.09 | 2.71 | 3.65 |
| $K_2O$ | 0.31 | 3.21 | 5.64 | 2.76 | 2.39 | 2.83 | 3.77 | 1.02 |
| $P_2O_5$ | 0.14 | 0.17 | 0.26 | 0.23 | 0.18 | 0.54 | 0.47 | 0.43 |
| LOI | 0.00 | 0.00 | 0.00 | 0.00 | 0.00 | 0.00 | 0.00 | 0.00 |
| Cr | 420 | 13 | 17 | 17 | 158 | 45 | 28 | 17 |
| Ni | 187 | 0 | 0 | 0 | 68 | 13 | 0 | 0 |
| Co | 41 | 0 | 0 | -5 | 19 | 19 | 23 | 14 |
| Sc | 22 | 6 | 5 | 7 | 20 | 25 | 29 | 15 |
| V | 163 | 66 | 67 | 67 | 135 | 249 | 316 | 179 |
| Cu | 53 | 0 | 0 | 0 | 33 | 57 | 86 | 11 |
| Pb | 2 | 4 | 18 | 4 | 6 | 12 | 13 | 13 |
| Zn | 61 | 20 | 50 | 42 | 86 | 79 | 90 | 70 |
| Bi | 0.00 | 0.00 | 0.00 | 0.00 | 0.32 | 0.00 | 0.00 | 0.31 |
| Cd | 0.00 | 0.00 | 0.00 | 0.00 | 0.00 | 0.00 | 0.00 | 0.00 |
| In | 0.00 | 0.00 | 0.00 | 0.00 | 0.07 | 0.05 | 0.00 | 0.00 |
| Sn | 1.13 | 0.84 | 2.80 | 0.86 | 2.22 | 1.15 | 2.19 | 0.94 |
| Mo | 0.00 | 0.53 | 0.31 | 0.32 | 0.21 | 0.00 | 0.00 | 0.21 |
| Sb | 0.00 | 0.21 | 0.31 | 0.00 | 0.53 | 0.31 | 0.52 | 0.63 |
| Ag | 0.0 | 0.0 | 0.0 | 0.0 | 0.0 | 0.1 | 0.0 | 0.1 |
| Rb | 4 | 86 | 166 | 78 | 80 | 105 | 125 | 30 |
| Cs | 0.09 | 2.73 | 3.32 | 2.90 | 3.49 | 3.98 | 6.27 | 1.46 |
| Ba | 170 | 851 | 1556 | 967 | 391 | 1676 | 2088 | 396 |
| Sr | 384 | 252 | 143 | 337 | 69 | 387 | 811 | 1063 |
| Tl | 0.00 | 0.52 | 0.58 | 0.41 | 0.45 | 0.41 | 0.45 | 0.15 |
| Ga | 14 | 14 | 19 | 16 | 18 | 20 | 24 | 17 |
| Ta | 0.86 | 1.26 | 1.35 | 0.95 | 1.04 | 0.82 | 1.04 | 0.76 |
| Nb | 15.9 | 16.8 | 22.8 | 15.0 | 16.9 | 17.8 | 17.8 | 14.6 |
| Hf | 1.59 | 3.68 | 5.19 | 3.33 | 6.55 | 4.09 | 5.01 | 3.23 |
| Zr | 63 | 137 | 187 | 118 | 232 | 168 | 188 | 146 |
| Y | 12 | 23 | 27 | 19 | 27 | 27 | 30 | 24 |
| Th | 0.87 | 23.12 | 30.07 | 25.78 | 10.57 | 33.52 | 20.88 | 15.64 |
| U | 0.26 | 1.26 | 5.50 | 2.04 | 2.01 | 6.18 | 6.06 | 4.07 |
| La | 8.61 | 64.12 | 81.92 | 82.72 | 40.15 | 119.41 | 100.24 | 46.92 |
| Ce | 19.27 | 115.62 | 155.55 | 150.41 | 82.42 | 199.02 | 187.95 | 96.97 |
| Pr | 2.38 | 12.61 | 17.63 | 17.19 | 9.72 | 22.00 | 21.93 | 11.47 |
| Nd | 10.31 | 44.15 | 61.18 | 58.01 | 39.10 | 78.56 | 78.31 | 45.88 |
| Sm | 2.49 | 8.09 | 9.85 | 9.45 | 7.19 | 12.57 | 13.57 | 8.34 |
| Eu | 0.90 | 1.68 | 2.28 | 2.36 | 1.48 | 3.14 | 3.34 | 1.98 |
| Gd | 2.83 | 5.78 | 7.05 | 6.55 | 5.81 | 8.59 | 10.02 | 6.57 |
| Tb | 0.46 | 0.79 | 0.91 | 0.80 | 0.89 | 1.15 | 1.25 | 0.85 |
| Dy | 2.49 | 3.99 | 4.56 | 3.55 | 4.75 | 5.13 | 5.95 | 4.27 |
| Ho | 0.46 | 0.70 | 0.79 | 0.61 | 0.96 | 0.88 | 1.03 | 0.71 |
| Er | 1.13 | 1.68 | 2.07 | 1.50 | 2.54 | 1.99 | 2.40 | 1.77 |
| Tm | 0.16 | 0.27 | 0.30 | 0.23 | 0.41 | 0.28 | 0.33 | 0.27 |
| Yb | 0.99 | 1.68 | 1.97 | 1.40 | 2.85 | 1.57 | 2.09 | 1.67 |
| Lu | 0.15 | 0.28 | 0.34 | 0.25 | 0.46 | 0.25 | 0.34 | 0.28 |
| Be | 0.00 | 2.00 | 4.25 | 2.58 | 1.58 | 4.40 | 5.33 | 2.61 |
| $Zr/TiO_2$ | 50.00 | 520.00 | 562.50 | 423.08 | 231.58 | 216.22 | 236.84 | 259.26 |
| Zr/Hf | 40.00 | 37.14 | 36.00 | 35.48 | 35.48 | 41.03 | 37.50 | 45.16 |
| Y/Zr | 0.20 | 0.17 | 0.14 | 0.16 | 0.12 | 0.16 | 0.16 | 0.16 |
| Nb/Y | 1.27 | 0.73 | 0.85 | 0.78 | 0.62 | 0.65 | 0.59 | 0.61 |